ployed by Bursten, Cotton, Hall, and co-workers. In their preceding published work dealing with trinuclear metallic clusters,[46-49] they emphasized the investigation of how the Mulliken population of the canonical valence orbitals of the metallic cluster varied with different ligand environments and analyzed the possible trend of metal-metal bond lengths. Many of our conclusions are similar. For instance, we have both deduced that the role of the terminal ligands is less important. Our study complements that of Bursten, Cotton, Hall, et al. These simplified models must be used with care. For instance, when each bidentate ligand is replaced by two terminal ligands, some frontier MO's, predominantly of ligand character, are automatically eliminated. Some fragment MO's that in the carboxylate were in the frontier MO region here are missing.

Acknowledgment. This work is an outcome of a joint USA-PRC research program supported by NSF Grant INT-8117267 and the Academia Sinica. Collaborating in this project are the groups of Lu Jiaxi, Tang Aoqing, James A. Ibers, and Roald Hoffmann. We are most grateful to F. A. Cotton, Z. Dori, and T. A. Albright for important comments, correcting some errors in an earlier version of this work.

Appendix

The experimental and idealized model geometrical parameters of $Mo_3S_2Cl_9^{3-}$ are listed in Table V.

Our calculations used the extended Hückel method,[53] with weighted H_{ij}'s.[54] The Coulomb integrals and wave functions are specified in Table VI.[55]

Registry No. 2, 92844-13-8.

(53) Hoffmann, R. *J. Chem. Phys.* **1963**, *39*, 1397.
(54) (a) Ammeter, J. H.; Bürgi, H.-B.; Thibeault, J. C.; Hoffmann, R. *J. Am. Chem. Soc.* **1978**, *100*, 3686. (b) Hoffmann, R.; Hoffmann, P. *Ibid.* **1976**, *98*, 598.
(55) Summerville, R. H.; Hoffmann, R. *J. Am. Chem. Soc.* **1976**, *98*, 7240.

Mechanisms of the Carbon–Hydrogen Bond-Forming Binuclear Reductive Elimination Reactions of Benzyl- and Hydridomanganese Carbonyls†

Mario J. Nappa, Roberto Santi, and Jack Halpern*

Department of Chemistry, The University of Chicago, Chicago, Illinois 60637

Received July 19, 1984

The reactions between $RMn(CO)_4L$ [R = *p*-$MeOC_6H_4CH_2$; L = CO (**1a**), L = (*p*-$MeOC_6H_4)_3P$ (**1c**)] and $HMn(CO)_4L$ [L = CO (**2a**), L = (*p*-$CH_3OC_6H_4)_3P$ (**2c**)] exhibit diverse stoichiometries and mechanistic pathways, depending upon the solvent and CO concentration and on whether L = CO or (*p*-$CH_3OC_6H_4)_3P$. The following reactivity patterns were identified: (1) In benzene: **1a** $\rightleftarrows$ $RMn(CO)_4$ + CO, followed by $RMn(CO)_4$ + **2a** $\rightarrow$ RH. (2) In acetonitrile or acetone (S): **1a** $\rightleftarrows$ $RCOMn(CO)_4(S)$, followed by $RCOMn(CO)_4(S)$ + **2a** $\rightarrow$ RCHO. (3) In benzene: **1c** $\rightarrow$ R· + ·$Mn(CO)_4P$, followed by R· + **2c** $\rightarrow$ RH. (4) In benzene: **1c** + CO $\rightarrow$ $RCOMn(CO)_4P$, followed by $RCOMn(CO)_4P$ + **2c** $\rightarrow$ RCHO. The kinetics of the reactions are described and the factors influencing the choice of reaction pathway discussed.

Binuclear reductive elimination reactions between transition-metal alkyls and transition-metal hydrides constitute important steps in a variety of stoichiometric and catalytic processes, for example, the product-forming steps in certain hydrogenation and hydroformylation reactions. However, only recently have such reactions received direct attention.[1] Several studies have revealed diverse reactivity patterns and led to disparate mechanistic conclusions; only in a few cases has an actual binuclear reductive elimination step been directly identified. Norton[1a] has reported that the thermal decomposition of $OsH(CH_3)(CO)_4$ is an intermolecular process and suggested that methane is formed by reductive elimination from a binuclear acyl hydride intermediate. He also reported similar reactivity patterns for reactions of iridium and rhodium acyls with osmium hydrides. More commonly, reductive elimination reactions between metal acyl and metal hydride complexes yield aldehydes. Recently, it has been suggested that the aldehyde-producing step in hydroformylation involves such a binuclear reductive elimination reaction between $RCOCo(CO)_4$ and $HCo(CO)_4$.[2] Inhibition of the reaction by CO suggests that this step involves a vacant coordination site.[3] Bergman[4] has reported that reaction between a molybdenum alkyl $CpMo(CH_3)(CO)_3$ and the corresponding hydride $CpMoH(CO)_3$ produces acetaldehyde through binuclear reductive elimination, following alkyl migration to generate a coordinatively unsaturated acyl complex. For the corresponding benzylmolybdenum complex, Mo–C bond homolysis apparently is competitive with alkyl migration and mixtures of aldehyde and toluene are formed.[4] Gladysz[5] has reported that $C_6H_5Mn(CO)_5$ reacts rapidly with

† Dedicated to the memory of Earl L. Muetterties.

(1) For recent reviews see: (a) Norton, J. R. *Acc. Chem. Res.* **1979**, *12*, 139. (b) Bergman, R. G. *Acc. Chem. Res.* **1980**, *13*, 113. (c) Halpern, J. *Inorg. Chim. Acta* **1982**, *62*, 31.
(2) Alemdaraglu, N. H.; Penninger, J. C. M.; Otlay, E. *Monatsh. Chem.* **1976**, *107*, 1153.
(3) Heck, R. F.; Breslow, D. S. *Chem. Ind. (London)* **1960**, 467. Heck, R. F. *Adv. Organomet. Chem.* **1966**, *4*, 243. Heck, R. F. "Organotransition Metal Chemistry"; Academic Press: New York, 1975; p 217.
(4) Jones, W. D.; Bergman, R. G. *J. Am. Chem. Soc.* **1979**, *101*, 5447.
(5) Tam, W.; Wong, W.-K.; Gladysz, J. A. *J. Am. Chem. Soc.* **1979**, *101*, 1589.

0276-7333/85/2304-0034$01.50/0

$HMn(CO)_5$ at room temperature to form benzaldehyde, apparently through a binuclear reductive elimination pathway.

When alkyl migration to coordinated CO is precluded or is slow, reactions between transition-metal alkyls and hydrides typically yield RH rather than RCHO. Renault et al.[6] have reported the rapid evolution of methane at ambient temperatures from the reaction between Cp_2ZrMe_2 and $CpMo(CO)_3H$. Kaesz[7] reported that $CH_3Mn(CO)_5$ and Cp_2MH_2 (M = Mo or W) or Cp_2ReH react at ambient temperatures to yield CH_4 and H_2, the fourth hydrogen of methane coming from a Cp ring. $MeAuPPh_3$ reacts with $HOs(CO)_4SiMe_3$ or $HMn(CO)_5$ to form CH_4.[1a] Reaction between a metal alkyl and a metal hydride has been suggested as the product-forming step in the hydrogenation of acrylamide catalyzed by $[HRuCl(PPh_3)_2]_2$.[8] Bergman[9] has recently reported that the hydrogenolysis of $CpCoMe_2(PPh_3)$ yields methane through a binuclear reductive elimination reaction between $CpCoMe_2PPh_3$ and $CpCoH_2PPh_3$.

We have previously communicated preliminary results of our studies on reactions between several benzylmanganese carbonyl (**1**) and hydridomanganese carbonyl complexes (**2**) that reveal the accessibility of several distinct mechanisms of C–H bond-forming reductive elimination.[10] In this paper we report more detailed results of our continuing studies on these and related systems.

p-$CH_3OC_6H_4CH_2Mn(CO)_4L$
1a, L = CO
1b, L = PMe_2Ph
1c, L = $(p$-$CH_3OC_6H_4)_3P$

$HMn(CO)_4L$
2a, L = CO
2b, L = $PEtPh_2$
2c, L = $(p$-$CH_3OC_6H_4)_3P$

p-$CH_3OC_6H_4CH_2Mn(CO)_4$ **3a** $C_6H_5CH_2Mn(CO)_5$ **4a**

$Mn_2(CO)_9L$
5a, L = $PEtPh_2$
5b, L = $(p$-$CH_3OC_6H_4)_3P$

p-$CH_3OC_6H_4CH_2(CO)Mn(CO)_3LY$
6a, L, Y = CO
6b, L = PMe_2Ph, Y = CO
6c, L, Y = PMe_2Ph
6d, L = solvent (S), Y = CO
6e, L = $(p$-$CH_3OC_6H_4)_3P$, Y = CO

$Mn_2(CO)_8L_2$
7a, L = $(p$-$CH_3OC_6H_4)_3P$
7b, L = $PMePh_2$

Results

Reactions of p-$CH_3OC_6H_4CH_2Mn(CO)_5$ (1a) with $HMn(CO)_5$ (2a) in Nondonor Solvents. The reaction of **1a** with **2a** in benzene yields p-$CH_3OC_6H_4CH_3$ according to eq 1. The mechanism of this reaction (eq 2–4) ap-

$$\mathbf{1a} + \mathbf{2a} \rightarrow p\text{-}CH_3OC_6H_4CH_3 + Mn_2(CO)_{10} \quad (1)$$

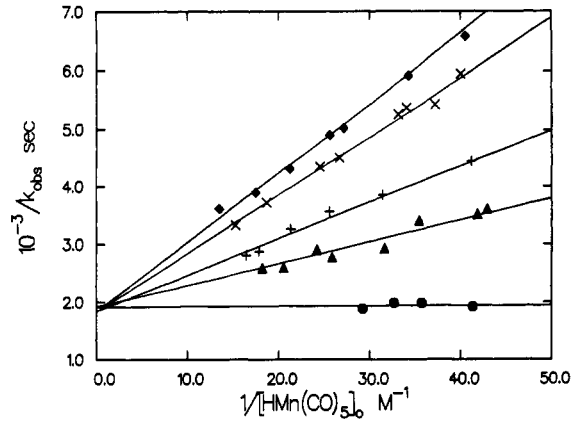

Figure 1. Plots of $1/k_{obsd}$ vs. $1/[HMn(CO)_5]_0$ for the reaction of **1a** with $HMn(CO)_5$ (eq 1) in benzene at 64.7 °C. CO partial pressures: ♦, 1 atm; ×, 0.75 atm; +, 0.50 atm; ▲, 0.25 atm; ●, 0 atm ([**1a**] = 4.7×10^{-3} M).

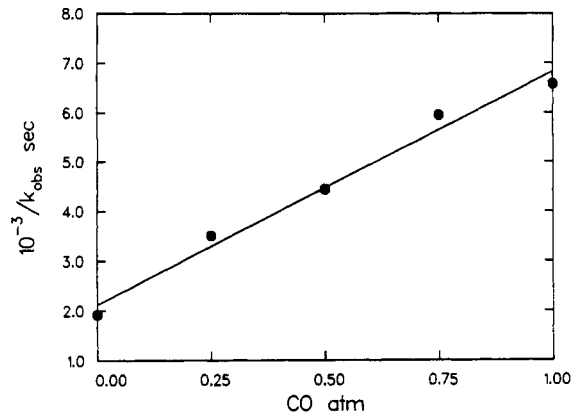

Figure 2. Plot of $1/k_{obsd}$ vs. CO partial pressure for the reaction of **1a** with $HMn(CO)_5$ in benzene at 64.7 °C.

parently involves initial dissociation of CO in accord with the rate law eq 5a which yields, upon rearrangement, eq 5b. Kinetic measurements, encompassing the initial

$$\mathbf{1a} \underset{k_{-2}}{\overset{k_2}{\rightleftharpoons}} \underset{\mathbf{3a}}{p\text{-}CH_3OC_6H_4CH_2Mn(CO)_4} + CO \quad (2)$$

$$\mathbf{3a} + \mathbf{2a} \xrightarrow{k_3} p\text{-}CH_3OC_6H_4CH_3 + Mn_2(CO)_9 \quad (3)$$

$$Mn_2(CO)_9 + CO \xrightarrow{\text{fast}} Mn_2(CO)_{10} \quad (4)$$

$$\frac{-\mathrm{d}\ln[\mathbf{1a}]}{\mathrm{d}t} = k_{obsd} = \frac{k_2k_3[\mathbf{2a}]}{k_{-2}[CO] + k_3[\mathbf{2a}]} \quad (5a)$$

$$\frac{1}{k_{obsd}} = \frac{k_{-2}[CO]}{k_2k_3[\mathbf{2a}]} + \frac{1}{k_2} \quad (5b)$$

concentration ranges $(2.5–5.4) \times 10^{-3}$ M **1a**, $(2.5–7.4) \times 10^{-2}$ M **2a**, and $(0–8.3) \times 10^{-3}$ M (0–1 atm) CO, yielded linear plots of $1/k_{obsd}$ vs. $1/[HMn(CO)_5]$ and $1/k_{obsd}$ vs. [CO] in accord with eq 5 (Figures 1 and 2). The slopes and intercepts of these plots yield the values $k_2 = (6.0 \pm 0.5) \times 10^{-4}$ s^{-1} and $k_{-2}/k_3 = 8.4 \pm 1.0$ at 65 °C.

Plausible mechanisms for step 3 include oxidative addition of **2a** to **3a** to form $[p$-$CH_3OC_6H_4CH_2MnH(CO)_4Mn(CO)_5]$, followed by *intramolecular* reductive elimination of p-$CH_3OC_6H_4CH_3$ or, alternatively, formation of a hydride-bridged intermediate analogous to that proposed for the formation of methane from $OsH(CH_3)(CO)_4$.[1a]

Attempts to intercept $Mn_2(CO)_9$ (eq 3) using rapid quenching techniques were unsuccessful. Phosphines

(6) Renault, P.; Tainturier, G.; Gautheron, B. *J. Organomet. Chem.* **1978**, *150*, C9.
(7) Hoxmeier, R. J.; Blickensderfer, J. R.; Kaesz, H. D. *Inorg. Chem.* **1979**, *18*, 3453. Hoxmeier, R. J.; Knobler, C. B.; Kaesz, H. D. *Inorg. Chem.* **1979**, *18*, 3462. Blickensderfer, J. R.; Hoxmeier, R. J.; Kaesz, H. D. *Inorg. Chem.* **1979**, *18*, 3606.
(8) James, B. R.; Wang, D. K. W. *J. Chem. Soc., Chem. Commun.* **1977**, 550.
(9) Janowicz, A. H.; Bergman, R. G. *J. Am. Chem. Soc.* **1981**, *103*, 2489.
(10) Nappa, M. J.; Santi, R.; Diefenbach, S. P.; Halpern, J. *J. Am. Chem. Soc.* **1982**, *104*, 619.

could not be used for this purpose because they react rapidly with $HMn(CO)_5$.

Kinetic measurements on the corresponding reaction of $C_6H_5CH_2Mn(CO)_5$ (**4a**) with $HMn(CO)_5$ yielded $\Delta H^* = 24.5 \pm 0.7$ kcal/mol and $\Delta S^* = -3.4 \pm 2.0$ cal/(mol K). A Hammett plot of the rate constants, k_2, for reactions between $HMn(CO)_5$ and several p-$XC_6H_4CH_2Mn(CO)_5$ derivatives (p-CH_3O, 6.0×10^{-4} s^{-1}; p-CH_3, 4.2×10^{-4} s^{-1}; H, 2.3×10^{-4} s^{-1}; p-Cl, 1.6×10^{-4} s^{-1}; p-CN, 1.0×10^{-4} s^{-1}, all in benzene at 65 °C)[11] yields $\rho = -0.57 \pm 0.08$, reflecting significant facilitation of CO loss by electron-donating substituents. Enhancement of the rate of CO dissociation by electron-donating substituents also has been observed by Pruett et al.[12] for the decarbonylation of a series of $XCH_2(CO)Mn(CO)_5$ complexes and interpreted in terms of stabilization of the coordinatively unsaturated intermediate resulting from CO loss. A similar rationale has been invoked by Heck[13] to account for the reactivity patterns of the reactions of $R(CO)Co(CO)_4$ with phosphines.

Reaction of **1a** with the less reactive hydride $HMn(CO)_4(PEtPh_2)$ (eq 6) yielded essentially the same value of k_2, $(5.4 \pm 0.3) \times 10^{-4}$ s^{-1} at 65 °C.

$$\mathbf{1a} + \underset{\mathbf{2b}}{HMn(CO)_4PEtPh_2} \rightarrow p\text{-}CH_3OC_6H_4CH_3 + \underset{\mathbf{5a}}{Mn_2(CO)_9(PEtPh_2)} \quad (6)$$

Because of the similar reactivities of **2a** and **2b**, it was possible to use the latter hydride in a ^{13}CO-labeling experiment. (**2a** could not be used for this purpose because of rapid CO substitution under the reaction conditions.[14]) Since reaction 2 is reversible and reaction 4 involves incorporation of CO into the product (**5a** when **2b** is used), reaction of **1a** with **2b** under ^{13}CO should give rise to multiple ^{13}CO incorporation into **5a**. In accord with this, mass spectral measurements on the product revealed cascading $n + 1$, $n + 2$, and $n + 3$ peaks for the fragments $Mn_2(CO)_4PEtPh_2^+$ and $Mn_2(CO)_5PEtPh_2^+$, indicating multiple ^{13}CO incorporation. (Unfortunately, the parent molecular ion $Mn_2(CO)_9(PEtPh_2)^+$ is unstable and was not detected.)

Further evidence for reaction 2 was obtained by reacting **1a** with PMe_2Ph. In accord with eq 7–12, p-$CH_3OC_6H_4CH_2Mn(CO)_4(PMe_2Ph)$, (**1b**), p-$CH_3OC_6H_4CH_2(CO)Mn(CO)_4(PMe_2Ph)$ (**6b**), and p-$CH_3OC_6H_4CH_2(CO)Mn(CO)_3(PMe_2Ph)_2$ (**6c**) were observed to form in yields that depended on the initial PMe_2Ph concentration.

$$\mathbf{1a} \underset{k_{-7}}{\overset{k_7}{\rightleftharpoons}} \mathbf{3a} + CO \quad (7)$$

$$\mathbf{1a} \xrightarrow{k_8} p\text{-}CH_3OC_6H_4CH_2(CO)Mn(CO)_4 \quad (8)$$

$$\mathbf{3a} + PMe_2Ph \xrightarrow{\text{fast}} \mathbf{1b} \quad (9)$$

$$p\text{-}CH_3OC_6H_4CH_2(CO)Mn(CO)_4 + PMe_2Ph \xrightarrow{\text{fast}} \mathbf{6b} \quad (10)$$

$$\mathbf{1a} + PMe_2Ph \xrightarrow{k_{11}} \mathbf{6b} \quad (11)$$

$$\mathbf{6b} + PMe_2Ph \xrightarrow{k_{12}} \mathbf{6c} \quad (12)$$

(11) Diefenbach, S. P.; Halpern, J., unpublished results.
(12) Cawse, J. N.; Fiato, R. A.; Pruett, R. L. *J. Organomet. Chem.* **1979**, *172*, 405.
(13) Heck, R. F. *J. Am. Chem. Soc.* **1963**, *85*, 651.
(14) Byers, B. B.; Brown, T. L. *J. Organomet. Chem.* **1977**, *127*, 181.

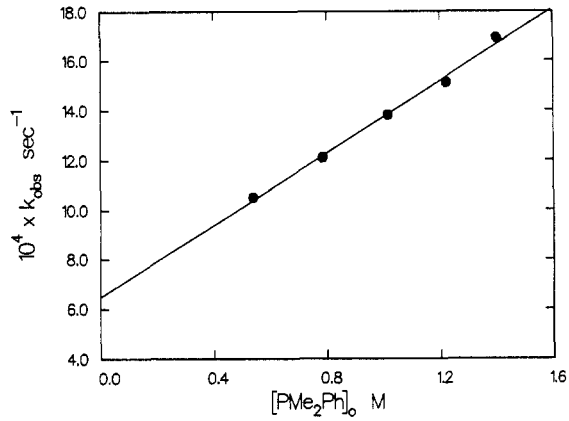

Figure 3. Plot of k_{obsd} vs. $[PMe_2Ph]_0$ for the reaction of **1a** with PMe_2Ph in C_6D_6 at 65 °C ($[\mathbf{1a}]_0 = (9.6\text{–}9.9) \times 10^{-2}$ M).

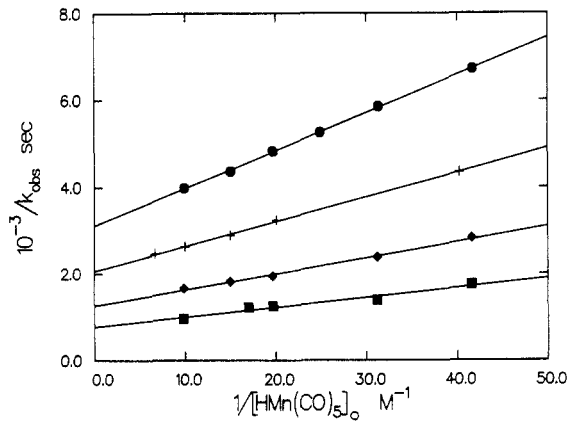

Figure 4. Plots of $1/k_{obsd}$ vs. $1/[HMn(CO)_5]_0$ for the reaction of **1a** with **2a** in acetone (eq 13) ($[\mathbf{1a}]_0 = 9.7 \times 10^{-4}$). Temperatures: ●, 20.1 °C; +, 25.6 °C; ♦, 29.9 °C; ■, 34.6 °C.

According to this scheme, the rate of reaction of **1a** is given by $-\mathrm{d} \ln [\mathbf{1a}]/\mathrm{d}t = k_{obsd} = k_7 + k_8 + k_{11}[PMe_2Ph]$. The linear plot of k_{obsd} vs. $[PMe_2Ph]$ in Figure 3 is consistent with this and yields $(k_7 + k_8) = 6.5 \times 10^{-4}$ s^{-1} at 65 °C. Comparison with the previously determined value of k_7 (6.0×10^{-4} s^{-1}) confirms that the "solvent-unassisted" migration of the benzyl group in **1a** (i.e., k_8) is very slow. The slope of Figure 3 yields $k_{11} = (7.3 \pm 0.3) \times 10^{-4}$ M^{-1} s^{-1} at 65 °C.

Reactions of p-$CH_3OC_6H_4CH_2Mn(CO)_5$ (1a) with $HMn(CO)_5$ (2a) in Donor Solvents. The reaction of **1a** with **2a** in acetone or acetonitrile (S) yields the aldehyde, p-$CH_3OC_6H_4CH_2CHO$ (identified by NMR), and $Mn_2(CO)_9S$ (identified by IR and vis/UV spectroscopy) according to the stoichiometry of eq 13. The kinetics of the reaction

$$\mathbf{1a} + \mathbf{2a} \xrightarrow{S} p\text{-}CH_3OC_6H_4CH_2CHO + Mn_2(CO)_9S \quad (13)$$

were found to conform to the mechanism of eq 14 and 15, yielding the rate law eq 16a, which rearranges to eq 16b.

$$\mathbf{1a} + S \underset{k_{-14}}{\overset{k_{14}}{\rightleftharpoons}} \underset{\mathbf{6d}}{p\text{-}CH_3OC_6H_4CH_2(CO)Mn(CO)_4S} \quad (14)$$

$$\mathbf{6d} + \mathbf{2a} \xrightarrow{k_{15}} p\text{-}CH_3O_6H_4CH_2CHO + Mn_2(CO)_9S \quad (15)$$

$$\frac{-\mathrm{d} \ln [\mathbf{1a}]}{\mathrm{d}t} = k_{obsd} = \frac{k_{14}k_{15}[\mathbf{2a}]}{k_{-14} + k_{15}[\mathbf{2a}]} \quad (16a)$$

$$\frac{1}{k_{obsd}} = \frac{k_{-14}}{k_{14}k_{15}[\mathbf{2a}]} + \frac{1}{k_{14}} \quad (16b)$$

The results of the kinetic measurements are reported in Table I. Linear plots of $1/k_{obsd}$ vs. $1/[HMn(CO)_5]$,

Table I. Kinetic Data for Reactions of 1a with 2a (Eq 13) in Donor Solvents

$10^4[1a]_0$, M	$10^2[2a]_0$,[a] M	$10^2[L]_0$,[b] M	solv	temp, °C	10^4k_{obsd},[c] s^{-1}
9.40	2.40	0	$(CH_3)_2CO$	20.1	1.49
9.40	3.20	0	$(CH_3)_2CO$	20.1	1.71
9.65	4.01	0	$(CH_3)_2CO$	20.1	1.90
9.68	5.07	0	$(CH_3)_2CO$	20.1	2.07
9.65	6.68	0	$(CH_3)_2CO$	20.1	2.29
9.65	10.0	0	$(CH_3)_2CO$	20.1	2.51
10.0	2.49	0	$(CH_3)_2CO$	25.6	2.30
10.0	4.97	0	$(CH_3)_2CO$	25.6	3.10
9.64	6.67	0	$(CH_3)_2CO$	25.6	3.47
9.46	9.97	0	$(CH_3)_2CO$	25.6	3.81
9.46	14.9	0	$(CH_3)_2CO$	25.6	4.06
9.45	2.40	0	$(CH_3)_2CO$	29.9	3.55
9.45	3.20	0	$(CH_3)_2CO$	29.9	4.20
9.45	5.07	0	$(CH_3)_2CO$	29.9	5.15
9.45	6.67	0	$(CH_3)_2CO$	29.9	5.48
9.45	10.1	0	$(CH_3)_2CO$	29.9	6.02
9.51	2.40	0	$(CH_3)_2CO$	34.6	5.72
9.51	3.20	0	$(CH_3)_2CO$	34.6	7.18
9.51	5.07	0	$(CH_3)_2CO$	34.6	7.99
9.51	5.87	0	$(CH_3)_2CO$	34.6	8.20
9.51	10.1	0	$(CH_3)_2CO$	34.6	10.4
9.90	0	2.83	$(CH_3)_2CO$	25.5	4.33
9.30	0	5.89	$(CH_3)_2CO$	25.5	4.43
9.30	0	11.8	$(CH_3)_2CO$	25.5	4.27
9.30	0	17.7	$(CH_3)_2CO$	25.5	4.34
9.59	2.40	0	CH_3CN	20.0	1.75
9.59	3.20	0	CH_3CN	20.0	1.89
9.59	5.07	0	CH_3CN	20.0	2.02
9.46	10.1	0	CH_3CN	20.0	2.15
9.58	2.40	0	CH_3CN	25.6	3.00
9.58	3.20	0	CH_3CN	25.6	3.28
9.58	5.07	0	CH_3CN	25.6	3.59
9.58	10.1	0	CH_3CN	25.6	4.03
9.48	2.40	0	CH_3CN	29.8	4.33
9.48	3.20	0	CH_3CN	29.8	4.76
9.48	5.07	0	CH_3CN	29.8	5.28
9.48	10.1	0	CH_3CN	29.8	5.73
9.55	0	3.03	CH_3CN	25.6	4.41
9.55	0	6.31	CH_3CN	25.6	4.53
9.55	0	18.9	CH_3CN	25.6	4.63

[a] In acetone the reactions were monitored by vis/UV at 505 nm and in acetonitrile at 458 nm. [b] L = PMe_2Ph; in acetone, the reactions were monitored by vis/UV at 365 nm and in acetonitrile at 355 nm. [c] ±0.01 s^{-1}.

Table II. Rate Constants for Reactions of 1a and 2a in Donor Solvents

temp, °C	solv	10^4k_{15},[a] s^{-1}	$10^2(k_{-14}/k_{15})$,[a] M
20.2	acetone	3.2	2.8
25.2	acetone	4.8	2.8
29.9	acetone	7.9	2.9
34.6	acetone	12.8	2.9
19.8	acetonitrile	2.3	0.7
25.6	acetonitrile	4.5	1.2
29.8	acetonitrile	6.4	1.1

[a] Calculated from data in Table I.

depicted in Figure 4 for experiments in acetone at four temperatures, yielded the values of k_{14} and k_{-14}/k_{15} in Table II and the activation parameters $\Delta H^{\ddagger}_{14}$ = 16.7 kcal/mol and $\Delta S^{\ddagger}_{14}$ = −18 ± 4 cal/(mol K) similar to activation parameters for other CO migratory insertion reactions.[15] The small values of the ratio k_{-14}/k_{15} reflect a strong preference for reaction of **6d** with the hydride **2a**. Similar kinetic measurements in acetonitrile (Table I) yielded the values of k_{14} and k_{-14}/k_{15} in Table II and the activation parameters $\Delta H^{\ddagger}_{14}$ = 17.8 ± 1.4 kcal/mol and $\Delta S^{\ddagger}_{14}$ = −14 ± 2 cal/(mol K).

k_{14} also was evaluated independently from kinetic measurements on the reaction of **1a** with PMe_2Ph (eq 17) that yielded the pseudo-first-order rate law eq 18 consistent with the mechanism of eq 19 and 20.

$$\mathbf{1a} + PMe_2Ph \rightarrow \mathbf{6b} \quad (17)$$

$$-\mathrm{d} \ln [\mathbf{1a}]/\mathrm{d}t = k_{19}[\mathbf{1a}] \quad (18)$$

$$\mathbf{1a} \xrightarrow{k_{19}} \mathbf{6d} \quad (19)$$

$$\mathbf{6d} + PMe_2Ph \xrightarrow{\text{fast}} \mathbf{6b} + S \quad (20)$$

Kinetic measurements in acetone, encompassing the initial concentration ranges (9.3–9.9) × 10^{-4} M **1a** and 2.8 × 10^{-2} to 17.7 × 10^{-2} M PMe_2Ph, yielded k_{19} = (4.3 ± 0.1) × 10^{-4} s^{-1} at 25 °C, in agreement with the value of k_{14} (4.8 × 10^{-1} s^{-1}) previously determined from kinetic measurements on reaction 13. As reported above, the rate constant k_{11} of the direct (presumably solvent-unassisted) reaction of PMe_2Ph with **1a** *in benzene* (eq 11) is 7.3 × 10^{-4} M^{-1} s^{-4} *at 65 °C*. This pathway can therefore be neglected for the reactions in donor solvents that were conducted at 20–35 °C.

The kinetics of the reactions between **1a** and PMe_2Ph also were measured in acetonitrile, and k_{18} was determined to be 4.5 × 10^{-4} s^{-1} at 25.6 °C, in agreement with the value of k_{14} determined for the reaction of **1a** with **2a** in the same solvent (Table I).

Reactions of *cis*-*p*-$CH_3OC_6H_4CH_2Mn(CO)_4[(p\text{-}CH_3OC_6H_4)_3P]$ (1c) with *cis*-$HMn(CO)_4[(p\text{-}CH_3OC_6H_4)_3P]$ (2c) in Nondonor Solvents. While the

(15) Calderazzo, F.; Cotton, F. A. *Inorg. Chem.* **1962**, *1*, 30.

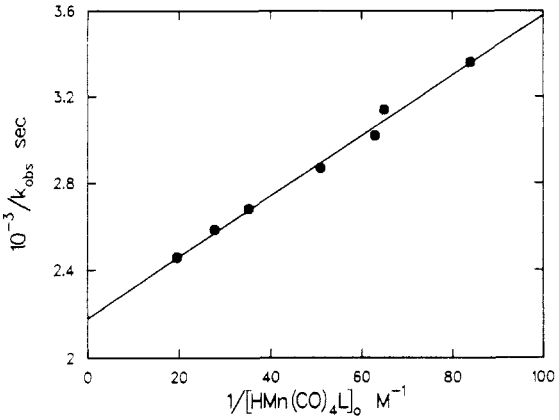

Figure 5. Plot according to eq 25b of $1/k_{obsd}$ vs. $1/[2c]_0$ for the reaction of **1c** with **2c** (eq 21) in C_6D_6 at 75.2 °C in the presence of 0.041 M **7a**.

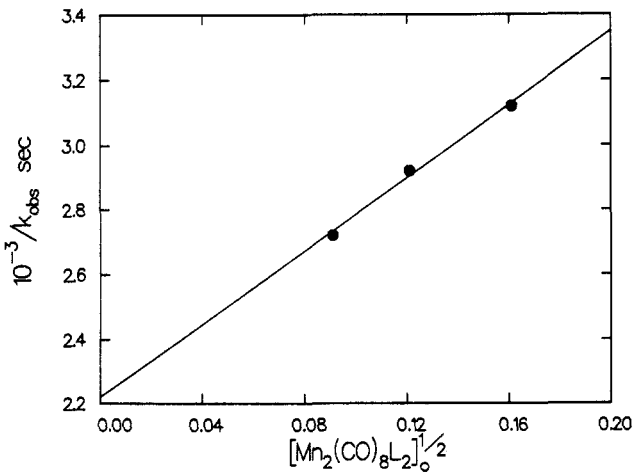

Figure 6. Plot according to eq 15b of $1/k_{obsd}$ vs. $[Mn_2(CO)_8P_2]^{1/2}$ for the reaction of **1c** with **2c** (eq 21) in benzene at 75 °C.

stoichiometry depicted by eq 21 parallels that of reaction 1, the reaction of **1c** with **2c** in benzene exhibited markedly different kinetics, consistent with the mechanism of eq 22–24 [P = $(p\text{-}CH_3OC_6H_4)_3P$] and the rate-law eq 25a that yields, upon rearrangement, eq 25b.

$$\mathbf{1c} + \mathbf{2c} \rightarrow p\text{-}CH_3OC_6H_4CH_3 + \underset{\mathbf{7a}}{Mn_2(CO)_8P_2} \quad (21)$$

$$\mathbf{1c} \underset{k_{-22}}{\overset{k_{22}}{\rightleftharpoons}} p\text{-}CH_3OC_6H_4CH_2\cdot + \cdot Mn(CO)_4P \quad (22)$$

$$p\text{-}CH_3OC_6H_4CH_2\cdot + \mathbf{2c} \xrightarrow{k_{23}} p\text{-}CH_3OC_6H_4CH_3 + \cdot Mn(CO)_4P \quad (23)$$

$$2\cdot Mn(CO)_4P \underset{k_{-24}}{\overset{k_{24}}{\rightleftharpoons}} \underset{\mathbf{7a}}{Mn_2(CO)_8P_2} \quad (24)$$

$$\frac{-\mathrm{d}\ln[\mathbf{1c}]}{\mathrm{d}t} = \frac{k_{22}k_{23}[\mathbf{2c}]}{k_{-22}(k_{-24}/k_{24})^{1/2}[\mathbf{7a}]^{1/2} + k_{23}[\mathbf{2c}]} \quad (25a)$$

$$\frac{1}{k_{obsd}} = \frac{k_{-22}(k_{-24}/k_{24})^{1/2}[\mathbf{7a}]^{1/2}}{k_{22}k_{23}[\mathbf{2c}]} + \frac{1}{k_{22}} \quad (25b)$$

Kinetic measurements in C_6D_6 (monitored by NMR), encompassing the initial concentration ranges 7.1×10^{-3} to 3.1×10^{-2} M **1c** and 9.1×10^{-2} to 3.3×10^{-1} M **2c** with no added **7a** (hence $k_{23}[\mathbf{2c}] >> k_{-22}(k_{-24}/k_{24})^{1/2}[Mn_2(CO)_8P_2]^{1/2}$ and $k_{obsd} \approx k_{22}$) yielded $k_{22} = (4.4 \pm 0.2) \times 10^{-4}$ s^{-1} at 75 °C.

In the presence of added **7a** (8.0×10^{-3} to 4.1×10^{-2} M), linear dependencies of $1/k_{obsd}$ on **[2c]** and on $[\mathbf{7a}]^{1/2}$ were observed (Figures 5 and 6) in accord with eq 25b. The slopes and intercepts of these plots yield $k_{22} = 4.6 \times 10^{-4}$ s^{-1} and $k_{-22}(k_{-24}/k_{24})^{1/2}/k_{23} = 3.2 \times 10^{-2}$ $M^{1/2}$ at 75 °C. With the assumption of diffusion-controlled values ($\sim 10^{10}$ M^{-1} s^{-1}) for k_{-22} and k_{24} and using the activation parameters reported by Poe[16] to calculate k_{-24} (0.16 s^{-1} at 75 °C), the value of k_{23} at 75 °C can be estimated to be 1.3×10^6 M^{-1} s^{-1}. This is consistent with the commonly observed facile hydrogen atom abstraction from a metal hydride by a carbon-centered free radical.[17] The activation parameters for the reactions of **1c** with various "radical traps" are listed in Table III. With the assumption of Mn–C bond homolysis to be the rate-determining step for these reactions, the Mn–C bond dissociation energy of **1c** can be estimated to be ca. 25–30 kcal/mol. This is in the range of other recently determined transition metal–alkyl bond dissociation energies.[18,19]

Table III. Activation Parameters for Reactions of 1c with Various Radical Traps

reaction	$\Delta H^{\ddagger}$, kcal/mol	$\Delta S^{\ddagger}$, cal/(mol K)
1c + **2c**[a]	27.4 ± 0.5	5 ± 1
1c + **2a**[b]	30.2 ± 0.5	13 ± 5
1c + O_2[c]	32.0 ± 1.5	19 ± 4

[a] Measured over the range 68.5–83.4 °C in C_6D_6 by NMR. [b] Measured over the range 65.0–75.0 °C in C_6D_6 by NMR. [c] Measured over the range 65.0–75.0 °C in toluene by IR.

Table IV. Reactions between 1c and 2a (Eq 26): Trapping of $\cdot Mn(CO)_4L$[a]

$[\mathbf{1c}]_0$, M	$[\mathbf{2a}]_0$, M	% **2c**[b]
0.026	0.30	77
0.023	0.60	87
0.025	0.90	90
0.025	1.20	94

[a] L = $(p\text{-}CH_3OC_6H_4)_3P$. [b] Percent of products derived from $\cdot Mn(CO)_4P(C_6H_4OCH_3)_3$. The % of **5b** was determined by vis/UV and the % of **2c** calculated by difference (% **2c** = 100 − % **5b**).

Reactions of *cis*-p-$CH_3OC_6H_4CH_2Mn(CO)_4[(p\text{-}CH_3OC_6H_4)_3P]$ (1c) with $HMn(CO)_5$ (2a). The reaction of **1c** with **2a** in benzene yields p-$CH_3OC_6H_4CH_3$, **2c**, and **5b** according to the stoichiometry of eq 26, consistent with the mechanistic scheme of eq 27–31. The pseudo-first-

$$\mathbf{1c} + (2-x)\mathbf{2a} \rightarrow p\text{-}CH_3OC_6H_4CH_3 + (1-x)\mathbf{2c} + (x)\mathbf{5b} + (1-x)Mn_2(CO)_{10}\ (0 < x < 1) \quad (26)$$

$$\mathbf{1c} \underset{k_{-22}}{\overset{k_{22}}{\rightleftharpoons}} p\text{-}CH_3OC_6H_4CH_2\cdot + \cdot Mn(CO)_4P \quad (27)$$

$$p\text{-}CH_3OC_6H_4CH_2\cdot + \mathbf{2a} \xrightarrow{\text{fast}} p\text{-}CH_3OC_6H_4CH_3 + \cdot Mn(CO)_5 \quad (28)$$

$$\cdot Mn(CO)_4P + \mathbf{2a} \xrightarrow{k_{29}} \mathbf{2c} + \cdot Mn(CO)_5 \quad (29)$$

$$2\cdot Mn(CO)_5 \xrightarrow{k_{30}} Mn_2(CO)_{10} \quad (30)$$

$$\cdot Mn(CO)_5 + \cdot Mn(CO)_4P \xrightarrow{k_{31}} \mathbf{5b} \quad (31)$$

(16) Jackson, R. A.; Poe, A. *Inorg. Chem.* **1978**, *17*, 997. Poe, A. *Inorg. Chem.* **1979**, *18*, 3331.
(17) Halpern, J. *Pure Appl. Chem.* **1979**, *11*, 2171.
(18) Halpern, J. *Acc. Chem. Res.* **1982**, *15*, 238.
(19) Connor, J. A.; Zafarani-Moattar, M. T.; Bickerton, J.; El Saied, N. I.; Suradi, S.; Carson, R.; Al Takhin, G.; Skinner, H. A. *Organometallics* **1982**, *1*, 1166.

Table V. Reactions of 1c with 2a under CO

$[1c]_0$, M	$[2a]_0$, M	CO, atm	$10^4 k_{obsd}$, s^{-1}	% RH[a]	% RCHO[a]
0.031-0.035	0.14-0.75	0	6.2	100	0
0.012	0.13-0.18	0.25	7.3	80	20
0.012-0.013	0.14-0.20	0.50	8.4	69	31
0.012-0.013	0.10-0.16	0.75	10.0	59	41
0.011-0.013	0.10-0.38	1.0	10.9	54	46

[a] Relative amounts determined by NMR.

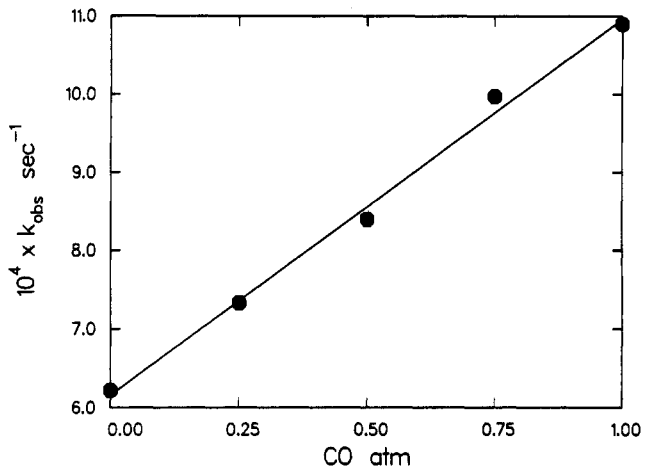

Figure 7. Plot of k_{obsd} vs. CO partial pressure for the reaction (eq 26) of 1c (1.1×10^{-2} to 3.5×10^{-2} M) with 2a ($(1.0\text{–}7.5) \times 10^{-2}$ M) in C_6D_6 at 75 °C.

order rate constant for this reaction, $k_{obsd} = -d \ln [1a]/dt$, was found to be $(5.4 \pm 0.2) \times 10^{-4}$ s^{-1} at 75 °C, somewhat higher than, but not incompatible with, the value of k_{22} (4.6×10^{-4} s^{-1}) previously determined from kinetic measurements on the reaction of 1c with 2c. While the value of k_{obsd} was independent of the concentration of 2a ($(2.2\text{–}7.5) \times 10^{-1}$ M), the product distribution did exhibit the dependence described by the data in Table IV. The partitioning of the products derived from $\cdot Mn(CO)_4P$ reflects its competing reactions with $\cdot Mn(CO)_4P$ and $\cdot Mn(CO)_5$ (eq 29 and 31). The possibility of a major contribution to the formation of 2c from a direct reaction of 5b with 2a was ruled out by determining k_{obsd} (= $-d \ln [5b]/dt$) for this reaction to be 4.1×10^{-5} s^{-1} at 75 °C, less than 10% of the rate constant (5.3×10^{-4}) for formation of 2c by reaction of 1c with 2a.

Further evidence for the proposed free radical mechanism was obtained from a crossover experiment between 1c and $Mn_2(CO)_8(PMePh_2)_2$ (7b) according to eq 32. The

$$1c + 7b \xrightarrow{k_{22}} \underset{2d}{p\text{-}CH_3OC_6H_4CH_2Mn(CO)_4PMePh_2} + \underset{7a}{Mn_2(CO)_8[P(p\text{-}CH_3OC_6H_4)_3]PMePh_2} \quad (32)$$

value of k_{obsd} (= $-d \ln [2c]/dt$) for this reaction (measured by NMR) was found to be 5.6×10^{-4} s^{-1} in C_6D_6 at 75.6 °C, in satisfactory agreement with the values of k_{22} measured by using other radical traps (2a, 5.4×10^{-4} s^{-1}; 2c, 4.6×10^{-4} s^{-1}; O_2, 7.1×10^{-4} s^{-1}). The slightly higher rate for O_2 may reflect a contribution from a direct reaction between 2c and O_2. The role of 7b as a radical trap in these experiments is consistent with its previously reported "weak" Mn–Mn bond (k for 7a → $2 \cdot Mn(CO)_4P$ was estimated to be 9.7×10^{-3} s^{-1} at 75 °C from the activation parameters for the reaction of 7b with O_2).[16]

Reaction of *cis*-*p*-$CH_3OC_6H_4CH_2Mn(CO)_4[(p\text{-}CH_3OC_6H_4)_3P]$ (1c) with $HMn(CO)_5$ (2a) in the Presence of CO. The reaction of 1c with 2a (which yields *p*-$CH_3OC_6H_4CH_3$ in the absence of CO) was examined under various CO partial pressures to test for a possible contribution from a path involving CO dissociation from 1c analogous to that for the corresponding reaction of 1a (eq 2). However, instead of suppressing the rate, it was found that CO accelerated the reaction of 1c with 2a due to a contribution from a path leading to the formation of aldehyde *p*-$CH_3OC_6H_4CH_2CHO$. The dependence of the product ratio [*p*-$CH_3OC_6H_4CH_3$]/[*p*-$CH_3OC_6H_4CH_2CHO$] on the CO partial pressure is reported in Table V. This behavior is consistent with the mechanistic scheme of eq 33–39 [P = $(p\text{-}CH_3OC_6H_4)_3P$].

$$1c \xrightarrow{k_{22}} p\text{-}CH_3OC_6H_4CH_2\cdot + \cdot Mn(CO)_4P \quad (33)$$

$$1c + CO \xrightarrow{k_{34}} \underset{6e}{p\text{-}CH_3OC_6H_4CH_2C(=O)Mn(CO)_4P} \quad (34)$$

$$p\text{-}CH_3OC_6H_4CH_2\cdot + 2a \xrightarrow{fast} p\text{-}CH_3OC_6H_4CH_3 + \cdot Mn(CO)_5 \quad (35)$$

$$6e \underset{k_{-36}}{\overset{k_{36}}{\rightleftharpoons}} p\text{-}CH_3OC_6H_4CH_2C(=O)\cdot + \cdot Mn(CO)_4P \quad (36)$$

$$p\text{-}CH_3OC_6H_4CH_2C(=O)\cdot + 2a \xrightarrow{fast} p\text{-}CH_3OC_6H_4CH_2CHO + \cdot Mn(CO)_5 \quad (37)$$

$$\cdot Mn(CO)_4P + 2a \xrightarrow{fast} 2c + \cdot Mn(CO)_5 \quad (38)$$

$$2 \cdot Mn(CO)_5 \xrightarrow{fast} Mn_2(CO)_{10} \quad (39)$$

This scheme yields k_{obsd} (= $-d \ln [1c]/dt$) = $k_{22} + k_{34}[CO]$ in accord with the linear plot of k_{obsd} vs. [CO] in Figure 7 that yields $k_{22} = 6.1 \times 10^{-4}$ s^{-1} (in agreement with previously determined values of k_{22}) and $k_{34} = 5.8 \times 10^{-2}$ M^{-1} s^{-1} at 75 °C. The latter value is considerably higher than the corresponding rate constant for the phosphine (PMe_2Ph) assisted benzyl migration reaction of 1a ($k_{11} = 7.3 \times 10^{-4}$ M^{-1} s^{-1} at 65 °C), reflecting enhancement by the coordinated phosphine $(p\text{-}CH_3OC_6H_4)_3P$, of the rate of migratory insertion. In the absence of phosphine ligands, e.g., in the reaction of *p*-$CH_3OC_6H_4CH_2Mn(CO)_5$ with $HMn(CO)_5$ under CO, migratory insertion does not occur. Such enhancement by phosphines and related ligands of migratory insertion has previously been reported for reactions of $IrEtCl_2(CO)_2L$ with L′ to form $Ir(COR)Cl_2(CO)LL'$ (L, L′ = $P(OPh)_3$, $AsMe_2Ph$, or PPh_3), the dependence of the rate on L being $P(OPh_3)_3$, PPh_3 >>> $AsMe_2Ph$ > $AsPh_3$.[20]

The above interpretation implies rapid reaction of 6e with 2a to generate *p*-$CH_3OC_6H_4CH_2CHO$ (eq 36 and 37). This was confirmed by direct measurement of the rate of reaction of 6e with excess 2a in C_6D_6 at 75 °C which yield exclusively *p*-$CH_3OC_6H_4CH_2CHO$ with a pseudo-first-order rate constant, k_{obsd} (= $-d \ln [6a]/dt$) of $(1.1 \pm 0.1) \times 10^{-3}$ s^{-1}, large enough so that 6e would not be observed as an intermediate in the reactions of 1c with 2a in the presence of CO. The formation of *p*-$CH_3OC_6H_4CH_2CHO$ requires

(20) Glyde, R. W.; Mawby, R. J. *Inorg. Chim. Acta* **1970**, *4*, 331.

the hydrogen abstraction step (eq 37) to be fast compared with decarbonylation of the p-$CH_3OC_6H_4CH_2\dot{C}O$ radical. The rate constant of decarbonylation of $C_6H_4CH_2\dot{C}O$ has been estimated to be ca. 5×10^7 s^{-1} at 25 °C.[21] A similar decarbonylation rate for p-$CH_3OC_6H_4CH_2\dot{C}O$ would require k_{37} to be greater than 5×10^8 M^{-1} s^{-1}. This is significantly higher than our estimate of ca. 1.3×10^6 M^{-1} s^{-1} for k_{23} but is not considered incompatible with the latter since **2a** is expected to be a much better H atom donor than **2c**. In accord with this, reaction between **6e** and **2c** was found to yield only p-$CH_3OC_6H_4CH_3$ and no p-$CH_3OC_6H_4CH_2CHO$!

Discussion

The number of characterized binuclear reductive elimination reactions between hydrido and alkyl transition-metal complexes is nearly matched by the variety of mechanisms that have been proposed for such reactions. These mechanisms (see Introduction) include (a) alkyl migration to coordinated CO followed by alkane elimination, (b) alkyl migration to coordinated CO followed by aldehyde elimination, (c) ligand (CO) dissociation followed by alkane elimination, (d) metal–alkyl bond homolysis followed by H atom abstraction leading to alkane formation, and (e) metal–acyl bond homolysis followed by H atom abstraction leading to aldehyde formation. The manganese carbonyl systems that are described in this paper have proven to be particularly versatile in respect of their reductive elimination reactions and have provided evidence for all of the above mechanistic pathways except (a).

Mechanism b has been identified for reactions between benzylmanganese carbonyl complexes **1a** and **4a** and $HMn(CO)_5$ in donor solvents such as acetone or acetonitrile. Other donor solvents are expected to exhibit similar behavior, notably DMF,[22] a solvent commonly used in hydroformylation and reported to be effective in promoting aldehyde formation, e.g., in the hydroformylation of formaldehyde.[23] The donor solvents apparently promote the formation of a solvent-stabilized acyl intermediate from which the donor solvent can be displaced by the hydride leading to aldehyde elimination. The hydride itself apparently is not a sufficiently good "donor" to promote alkyl migration, since no aldehyde is observed in reactions between **1a** and **2a**, even at high **2a** concentrations, in poor donor solvents such as benzene.

In the absence of phosphine ligands, i.e., for **1a**, migratory insertion apparently is slow in poor donor solvents such as benzene, while CO dissociation is rapid, so that mechanism c prevails. The coordinatively unsaturated manganese alkyl **3a** reacts rapidly with manganese hydride **2a** or **2c** to form p-$CH_3OC_6H_4CH_2CH_3$. Thus, by changing the solvent, the organic product selectivity can be completely altered.

We also have shown that for benzyl- and acylmanganese carbonyls, metal–carbon bond homolysis can become competitive with CO dissociation if a carbonyl ligand is replaced by a phosphine (mechanisms d and e). On the basis of the activation parameters that we have determined, the influence of phosphine substitution may be twofold, namely, (1) suppression of CO dissociation, presumably by increasing the electron density on the manganese and stabilizing the manganese–carbonyl bonds through enhanced π-back-donation and (2) acceleration of manganese–alkyl bond homolysis by steric distabilization.[24] Evidence for the former effect is provided by failure to observe any CO loss from **1c** even at 75 °C, compared with the rapid loss of CO from **1a**. Evidence for the latter effect may be deduced from the fact that, on the basis of the activation parameters measured for the homolysis of the Mn–C bond of **1c**, the rate constant calculated at 65 °C would be ca. 30% of the overall rate measured for the reaction of **1a** with **2a**. Since there is no detectable contribution from homolysis in the latter reaction, its contribution to the reaction of **1c** must reflect Mn–C bond weakening by the phosphine ligand. In line with this, it has also been reported that *cis*-$C_6H_5CH_2COMn(CO)_4PPh_3$ is unstable at room temperature.[25]

Although the evidence concerning the reaction between **6e** and **2a** is not as conclusive as for the other reactions, the results suggest that Mn–acyl bond homolysis is a step in the aldehyde-forming reaction. Under the high CO pressures of cobalt carbonyl catalyzed hydroformylation conditions, where CO dissociation from an acyl–cobalt intermediate is expected to be suppressed, this may well be an important pathway for aldehyde formation.

In summary, four distinct pathways have been identified for carbon–hydrogen bond-forming reductive elimination reactions of benzylmanganese carbonyls with hydridomanganese carbonyls. Relatively modest changes in ligands, solvent, or CO concentration may result in essentially complete crossover from one pathway to another. This underscores the danger of assuming mechanisms for such reactions in the absence of appropriate supporting evidence or of extrapolating from one reaction or set of conditions to another, even closely related, one. While some of the factors influencing the choice of pathways in such reactions have been identified, further elucidation of these factors clearly is warranted.

Experimental Section

General Data. NMR spectra were recorded on Bruker 90 and 270 MHz spectrometers; all chemical shifts are referenced to internal hexamethyldisilane (HMDS). IR spectra were recorded on a Perkin-Elmer 283 spectrophotometer. UV/vis measurements were made with either a GCA McPherson EU-700 or a Cary 14 spectrophotometer, equipped with a thermostated cell holder and connected to a recirculating constant temperature bath (±0.2 °C). All manipulations were carried out under a nitrogen atmosphere unless otherwise noted. THF, benzene, toluene, and diethyl ether were distilled from sodium benzophenone. C_6D_6 was distilled from sodium, and CD_3CN and $(CD_3)_2CO$ were degassed on a high vacuum line. Pentane, hexane, heptane, and methylene chloride were purged with nitrogen prior to use.

All kinetic measurements were made under pseudo-first-order conditions, generally with the hydride in substantial excess.

Reactions of 1 with 2. NMR. Air-stable **1a** or **1c** was weighed directly into an NMR tube. In a large Schlenk vessel under nitrogen, **2a**, HMDS, and deuterated solvent were added to the NMR tube by syringe and the tube was capped under nitrogen. In some cases, the NMR tubes were sealed under vacuum. Samples were heated to a constant temperature bath (±0.2 °C), and the reaction progress was monitored periodically by NMR at room temperature following the benzyl CH_2 resonance (δ 2.20 for **1a** and δ 2.16 for **1c** (J_{P-H} = 6 Hz)) in C_6D_6.

IR. Reactions were conducted in Schlenkware. For reactions studied under CO, prior to adding **2a** the solution was purged with a CO/N_2 gas mixture (25%, 50%, and 75% CO in N_2; Matheson Gas Products) for 10 min and then was kept under a hydrostatic head (ca. 10 mmHg) of gas mixture. The reaction was sampled periodically and the reaction progress monitored by IR (A_1 band

(21) Brunton, G.; McBay, H. C.; Ingold, K. U. *J. Am. Chem. Soc.* **1977**, *99*, 4447.
(22) Pruett, R. L. *Adv. Organomet. Chem.* **1971**, *17*, 31.
(23) Spencer, A. *J. Organomet. Chem.* **1980**, *194*, 113.
(24) Ng, F. T. T.; Rempel, G. L.; Halpern, J. *Inorg. Chim. Acta* **1983**, *77*, L165.
(25) Drew, D.; Darensbourg, M. Y.; Darensbourg, D. J. *J. Organomet. Chem.* **1975**, *85*, 73.

of **1a**, 2108 cm^{-1}). The solubilities of CO were estimated from the literature data[26] that were fitted to a second-order polynomial to yield a value of 0.239 for the Ostwald coefficient at 75 °C. The gas mixtures were analyzed as described.[27]

UV/vis. **1a** was added to a volumetric flask equipped with a side-arm stopcock. Degassed solvent was added under nitrogen. The solution of **1a** was then transferred to previously degassed 1-cm quartz cells fitted with rubber septa, and the liquid reactants were added directly to the cells by calibrated syringe.

Reactions of *cis*-1c with 2a. The rate constants were determined as described above. The yields of **2c** were determined spectrophotometrically. The extinction coefficients for $Mn_2(CO)_{10}$ and **5b** were determined at two wavelengths (345 and 360 nm) along with ϵ at λ_{max} for each compound (361 nm, **5b**; 343 nm, $Mn_2(CO)_{10}$). Reactions were followed for 5 half-lives in C_6D_6 in NMR tubes. C_6D_6 and **2a** were removed by vacuum, and the remaining solid was dissolved in benzene and transferred under nitrogen to a 25-mL volumetric flask. From absorbance measurements at two wavelengths (345 and 360 nm), the concentration of **5b** and the concentration of **2c**, by difference, were calculated. The UV/vis measurements were found to be in qualitative agreement with but more accurate than the NMR measurements.

Reaction of 1c with 7b (Crossover Experiment). **1c** (7.0 mg, 1.1×10^{-2} mmol) and **7b** (41.1 mg, 5.6×10^{-2} mmol) were weighed into an NMR tube under nitrogen. HMDS (2.0 μL) and degassed C_6D_6 were added for a total volume of 525 μL. The tube was capped and placed in a constant temperature bath at 75.6 ± 0.2 °C. Room-temperature NMR spectra were recorded at 0, 5, 10, 15, 20, 25, 35, 45, and 65 min.

Synthesis of 2a. $Mn_2(CO)_{10}$ (3.0 g, 7.7 mmol) was reacted with Na/Hg (600 mg/6 mL) in THF (60 mL). After 2 h, the mixture was filtered and dried and the white sodium salt washed with pentane for up to 12 h to remove occluded THF. The mixture was filtered again, vacuum dried, and reacted with degassed 85% H_3PO_4 (30 mL) and distilled onto P_2O_5. It was redistilled on a high vacuum line and collected in a *m*-xylene trap (−48 °C) to remove any residual THF; yield 2.41 g, 80%.

Synthesis of 1a. $Mn_2(CO)_{10}$ (1.99 g, 5.10×10^{-2} mmol) was reacted for 2 h at room temperature with Na/Hg (402 mg/4 mL) in THF (40 mL) and then filtered to afford a clear pale yellow solution. *p*-$CH_3OC_6H_4CH_2Cl$ (1.68 g, 1.08×10^{-2} mmol) dissolved in THF (15 mL) was added dropwise. This was stirred overnight and filtered and the THF removed by high vacuum. The solid was dissolved in pentane (100 mL) and filtered. This solution was reduced in volume and cooled to −20 °C for 24 h. The flask was then cooled to −78 °C and the mixture filtered and washed with cold pentane (2 × 10 mL at −78 °C): yield 1.78 g, 53%; ^1H NMR (C_6D_6, 270 MHz) δ CH_2Mn, 2.20 (s), CH_3O, 3.25 (s), $C_6H_{a_2}H_{b_2}$, 6.70 (d), 6.96 (d, J_{ab} = 8.5 Hz); IR (pentane, cm^{-1}) 2108 (w), 2014 (vs), 1994 (s).

Synthesis of 2b. $HMn(CO)_5$ (431 mg, 2.20 mmol) and $PEtPh_2$ (471 mg, 2.20 mmol) were reacted in hexane (12 mL) for 2 h. THF was removed by vacuum leaving an oil that was dissolved in pentane. The volume of the solution was reduced until a precipitate formed and then cooled to −20 °C for 2 days: yield 450 mg, 96%; IR (pentane, cm^{-1}) 2064 (w), 1987 (s), 1967 (s), 1956 (s).

Synthesis of *cis*-6e. **1a** (0.63 g, 2.0 mmol) and (*p*-$CH_3OC_6H_4)_3P$ (0.71 g, 2.0 mmol) were reacted in THF (25 mL) for 6 h. The THF was removed by vacuum, and the crude yellow solid (~400 mg) was purified by preparative TLC (2 mm SG; 80:20 CH_2Cl_2/hexane). The major band was collected, washed with CH_2Cl_2, and rotovapped to dryness to give a light yellow solid, yield 50 mg, 3.7%.

Synthesis of 5b. Toluene (60 mL) containing $Mn_2(CO)_{10}$ (1.0 g, 2.6 mmol) and (*p*-$CH_3OC_6H_4)_3P$ (2.7 g, 7.7 mmol) were refluxed for 16 h. THF was removed by vacuum and the solid chromatographed on Florisil (100–200 mesh) eluting with toluene/hexane (50:50). An oil was obtained from stripping the fast moving orange layer and was recrystallized at −20 °C from heptane/benzene (2:1): yield 470 mg, 0.66 mmol; IR (hexane, cm^{-1}) 2092 (m), 2013 (m), 1995 (s), 1974 (w), 1937 (w).

Synthesis of 7a. Toluene (70 mL) containing $Mn_2(CO)_{10}$ (980 mg, 2.5 mmol) and (*p*-$CH_3OC_6H_4)_3P$ (1.23 g, 3.5 mmol) was refluxed in a foil wrapped flask for 17 h. An oil obtained by removing the toluene in vacuo was chromatographed on florisil (100–200 mesh) eluting with toluene/hexane (50:50) and then toluene; yield 1.04 g, 40%.

Synthesis of 7b. $Mn_2(CO)_{10}$ (1.95 g, 5.0 mmol) and $PMePh_2$ (1.0 g, 5.0 mmol) in benzene (40 mL) were irridiated at ambient temperature with a 100-W Hanovia UV lamp for 9 h. Benzene was removed in vacuo and the residue crystallized from ethanol and then diethyl ether/ethanol; yield 2.20 g, 60%.

Synthesis of *cis*-2c. **2a** (1.28 g, 2.0 mmol) and (*p*-$CH_3OC_6H_4)_3P$ (0.22 g, 2.0 mmol) were dissolved in CH_2Cl_2 (25 mL). Trimethylamine *N*-oxide dihydrate (Aldrich, 267 mg, 2.4 mmol) was added to the solution while being stirred. After 3 h the CH_2Cl_2 was removed in vacuo and the residue purified by preparative TLC (2 mm SG; 80:20 CH_2Cl_2/hexane); yield 0.90 g, 70%.

Synthesis and Characterization of $Mn_2(CO)_9S$ (S = Acetone or Acetonitrile). [$Mn_2(CO)_9$(acetonitrile)]. $HMn(CO)_5$ (0.75 mmol) and **1a** (0.75 mmol) were dissolved in degassed CH_3CN (10 mL). The solution was stirred for 3 h and CH_3N removed by vacuum. The residue from the reaction was dissolved in CH_2Cl_2/hexane and chromatographed under nitrogen on neutral alumina using CH_2Cl_2/hexane (10:90, 400 mL) and then CH_2Cl_2/hexane (25:75, 400 mL). A yellow orange band was collected and the solid residue from solvent evaporation recrystallized from CH_2Cl_2/hexane (−78 °C): mp 96.0 °C; IR (hexane, cm^{-1}) 2095 (w), 2027 (m), 2007 (m), 1990 (b s), 1965 (w), 1949;[15] vis/UV (hexane) 347 nm (10 000 cm^{-1} M^{-1}), 408 (4200).

[$Mn_2(CO)_9$(acetone)]. A reaction similar to the one carried out in acetonitrile was carried in acetone, but the product was not stable in hexane and decomposed slowly yielding $Mn_2(CO)_{10}$ and a yellow insoluble solid: IR (hexane, cm^{-1}) (a) $Mn_2(CO)_9(acetone)_{ax}$, 2048, 2016, 1985, (b) $Mn_2(CO)_9(acetone)_{eq}$, 2094, 2026, 2005, 1989, 1964, 1947; vis/UV (acetone) 460 nm (~4500 cm^{-1} M^{-1}).

Acknowledgment. This research was supported by a grant from the National Science Foundation. The NMR facilities were supported in part through the University of Chicago Cancer Center Grant NIH-CA-14599. R.S. thanks the Montedison Donegani Institute for a leave of absence. M.J.N. thanks Du Pont for providing time for preparation of this paper.

Registry No. **1a**, 80105-78-8; **1b**, 92816-71-2; *cis*-**1c**, 80105-79-9; **2a**, 16972-33-1; **2b**, 92816-72-3; *cis*-**2c**, 80105-80-2; **4a**, 14049-86-6; **5a**, 92816-73-4; **5b**, 92816-74-5; **6b**, 92816-75-6; **6c**, 92816-76-7; *cis*-**6e**, 92816-77-8; **7a**, 15662-85-8; **7b**, 63393-52-2; $NaMn(CO)_5$, 13859-41-1; $Mn_2(CO)_9S$ (S = acetonitrile), 26595-04-0; $Mn_2(CO)_9S$ (S = acetone), 92816-78-9; $Mn_2(CO)_{10}$, 10170-69-1; *p*-$CH_3OC_6H_4CH_2Cl$, 824-94-2; *p*-$ClC_6H_4CH_2Mn(CO)_5$, 65982-69-6; *p*-$CNC_6H_4CH_2Mn(CO)_5$, 64491-83-4; *p*-$MeOC_6H_4CH_3$, 104-93-8; *p*-$MeOC_6H_4CH_2CHO$, 5703-26-4.

(26) Seidel, A.; Linke, W. F. "Solubilities of Inorganic and Metal-Organic Compounds", 4th ed.; D. Van Nostrand: New York, 1958; Vol. I.
(27) Lilburne, M. T. *Analyst (London)* **1966**, *91*, 571.